Topographically Induced Drag and Mixing at a Small Bank on the Continental Shelf

J. N. MOUM AND J. D. NASH

College of Oceanic and Atmospheric Sciences, Oregon State University, Corvallis, Oregon

(Manuscript received 14 June 1999, in final form 29 September 1999)

ABSTRACT

Recent turbulence measurements over a small bank on the continental shelf off Oregon reveal a previously undetected site for intense mixing of the coastal ocean. The flow is hydraulically controlled and turbulence diffusivities over the bank are more than 100 times greater than estimates made on the shelf away from topography. The total drag exerted by the bank on the flow field is a combination of bottom friction plus form drag (analogous to mountain drag) and is comparable to the Coriolis force. This drag is sufficient to decelerate the flow over the bank in a matter of hours.

1. Introduction

Few measurements of mixing along the continental shelf have been made, and only in regions of gradually varying topography (Crawford and Dewey 1989; Zülicke et al. 1998). These have led to the conclusion that mixing along the shelf is not much greater than that in the open ocean's main thermocline (Ledwell et al. 1993). Regions of extreme topography, such as submarine canyons and seamounts, are known to enhance mixing by at least an order of magnitude (Lueck and Osborn 1985; Lueck and Mudge 1997; Toole et al. 1997). However, little attention has been paid to the role of the numerous, though less extreme, topographic features along the continental shelf that rise to depths where they can interact with the dominant shelf flows.

2. Observations

An example of a small topographic feature on the continental shelf is Stonewall Bank, which rises 20 m above the 60-m-deep shelf off Newport, Oregon (Fig. 1). It is about 10 km long by 2 km wide and oriented NNW–SSE. Stonewall Bank is an important local bottom fishery. It is a rocky outcrop on a shelf that is predominantly silt and sand. Typically, an equatorward coastal jet dominates mean summer currents over the shelf (Huyer 1983). Strongly baroclinic tides (0.2–0.3 m s^{-1}) modulate the current structure and can produce large vertical shear (Pillsbury et al. 1974).

In April 1998, we executed a survey of currents, density, and turbulence above Stonewall Bank using a shipboard acoustic Doppler current profiler and by running our turbulence profiler, Chameleon (Moum et al. 1995), to within 2 cm of the bottom, using a protective ring to shield sensors. These detailed measurements revealed a complex and rapid evolution of flow structure and turbulent mixing over the bank.

Following the subsidence of sustained (>15 kt) northerly winds, a series of transects were made in a generally northeast to southwest direction across the bank. Observations from a single transect are shown in Fig. 2 as a density front reached the crest of the bank from the east. It was subsequently observed to flow over the bank and down the west side. The flow above the density front was nearly stagnant. Below 30 m, isopycnals were depressed downstream relative to upstream. A sharp rebound of isopycnals 24.6, 24.8 was observed at ~0.8 km.

Intense turbulence was produced in three distinct regions of the flow (Fig. 2): (i) along the bottom in a boundary layer formed by the flow of the bottom current; (ii) at the top of the bottom current where isopycnals were compressed and the vertical gradient in velocity was large, indicating a potential site of shear flow instability; and (iii) downstream of the bank crest, in association with an internal hydraulic jump.

3. Internal hydraulic control

The structure of the flow depicted in Fig. 2 is typical of a stratified hydraulic flow in which the upstream subcritical flow becomes supercritical downstream (Fig. 3; see Farmer and Denton 1985). Farther downstream, a transition from super- to subcritical flow (conversion of kinetic to potential energy in the form of an internal hydraulic jump) is associated with the raised interface

Corresponding author address: Dr. Jim Moum, College of Oceanic and Atmospheric Sciences, Oregon State University, 104 Ocean Administration Building, Corvallis, OR 97331-5503.
E-mail: moum@oce.orst.edu

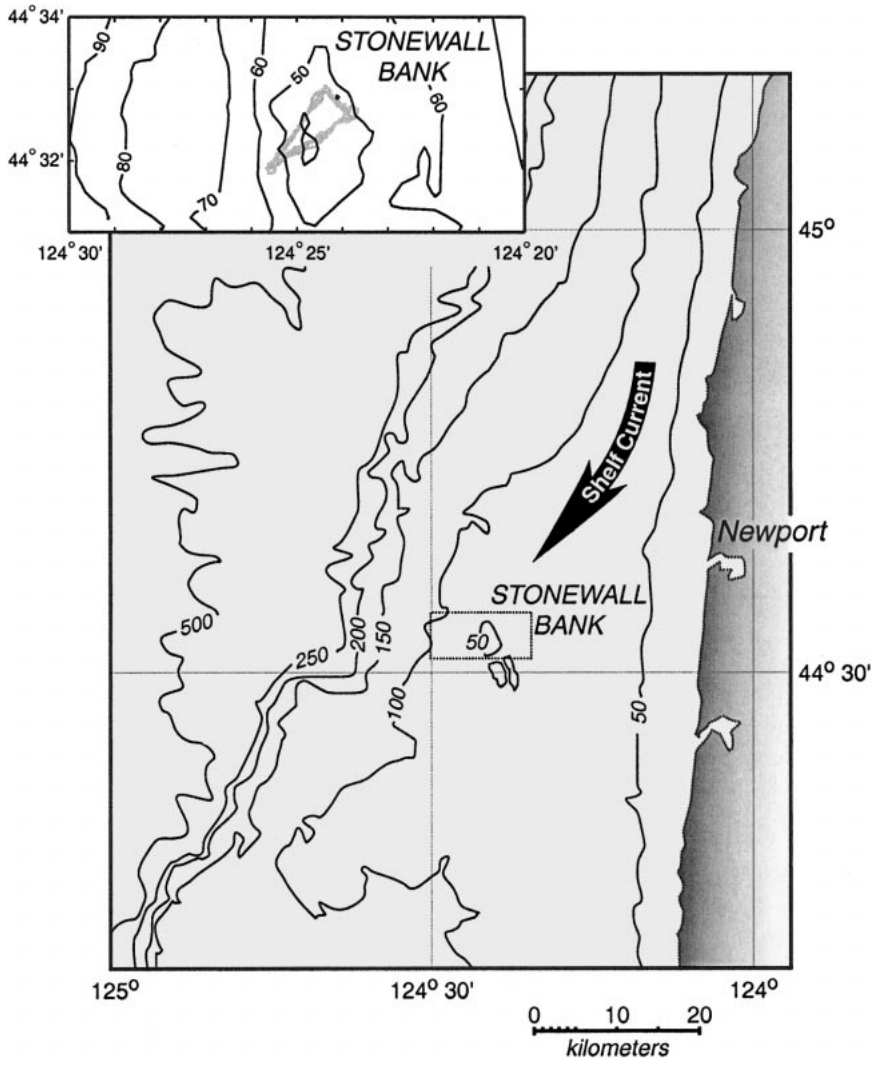

FIG. 1. Bathymetry of the coast near Stonewall Bank. The course of R/V *Wecoma* over the northern portion of Stonewall Bank is shown in the inset.

between upper and lower layers, spreading isopycnals, and turbulent mixing.

In the case of a two-layer flow, the flow hydraulics are characterized by the composite internal Froude number $G^2 = F_1^2 + F_2^2$, where $F_i^2 = q_i^2/g'h_i^3$, q_i is the flow rate per unit width, h_i is the layer thickness, and $g' = g(\rho_2 - \rho_1)/\rho_2$ is the reduced gravitational acceleration. The interface between the two layers is conveniently defined by the high stratification between the 24.4 and 24.6 isopycnals. For a stagnant upper layer, $F_1^2 = 0$. Two solutions (**ABC** and **ABD** in Fig. 3) produce flows that are critical ($G^2 = 1$) at the crest and subcritical ($G^2 < 1$) upstream. Downstream of the crest, the location of the observed interface suggests that it follows the supercritical ($G^2 > 1$) branch **BD**. By prescribing the downstream location of the jump and conserving momentum across the jump, the energy loss due to the transition from supercritical flow can be determined from the Bernoulli function evaluated between the point of departure from **BD** and a location downstream of the jump. Kinetic energy of the bottom flow is inefficiently lost to raising the interface, and turbulence ensues. The transition indicated by **E** releases 35 J m^{-3}; this compares well to both the measured integrated dissipation (30 J m^{-3}) and the observed interface height at **E**. Presumably, most of the energy lost from the flow at the jump goes to turbulent dissipation and mixing. Additional energy may be released through radiated gravity waves, which were not measured (Bacmeister and Pierrehumbert 1988).

4. Flow drag

The drag exerted by Stonewall Bank on the flow over it can be considered to be the sum of skin friction (due to dissipative losses in the bottom boundary layer) and

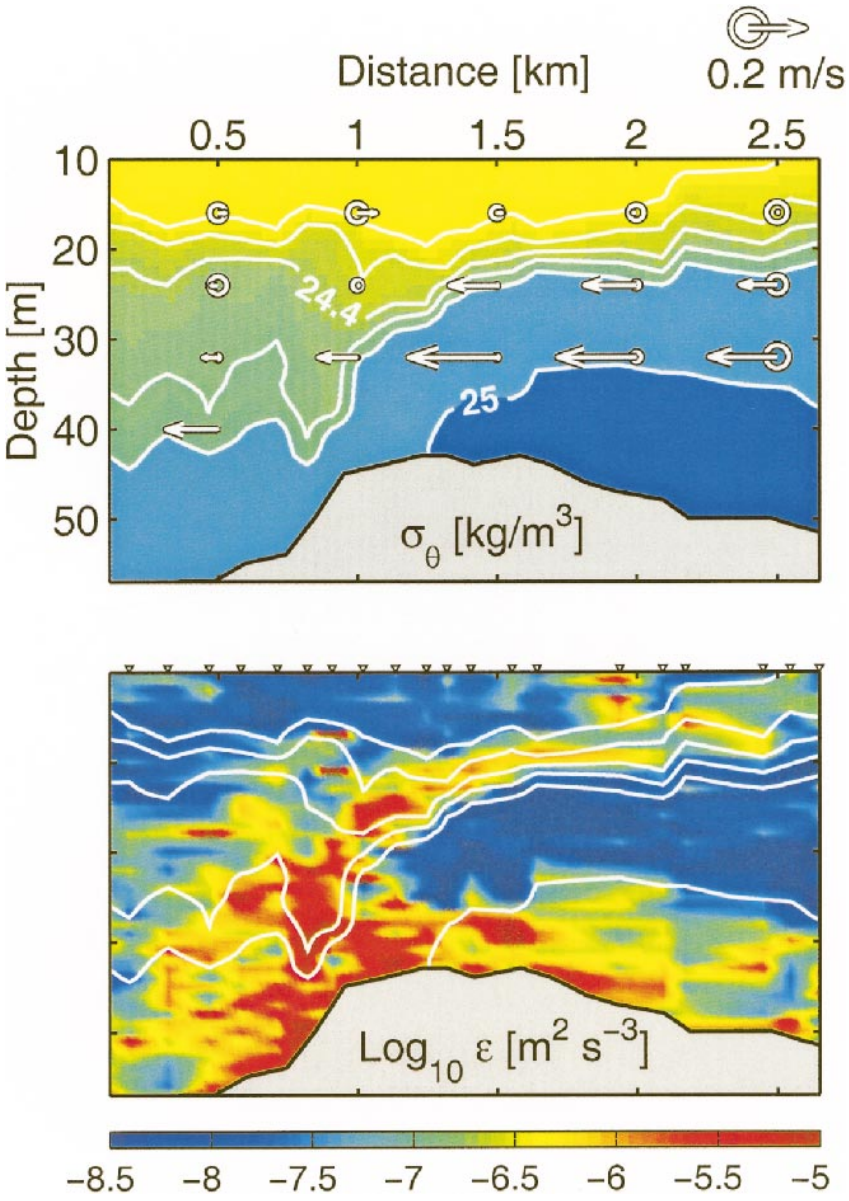

FIG. 2. (upper panel) Potential density ($\sigma_\theta = \rho$ [kg m^{-3}] $-$ 1000) across Stonewall Bank from one of 13 transects made in Apr 1998. Velocities derived from acoustic Doppler current profiler (ADCP) are indicated: arrows represent currents parallel to our transect; circles represent the velocity component out of the page (scale is shown above). Distance is measured relative to the southwest waypoint of our triangular course (Fig. 1). (lower panel) Turbulent dissipation rate, ϵ. Contours of potential density show the relationship between ϵ and the location of the front. Small triangles above plot indicate locations of individual vertical profiles.

form drag (associated with the pressure drop across the bank).

The bottom boundary layer was energetic, well mixed, and ranged from 1 to 15 m thick. The friction velocity u_* (the magnitude of turbulent velocities) was calculated assuming wall-layer scaling of the flow over the bottom. In the wall layer the bottom stress τ_b is constant and equal to ρu_*^2. The mean friction velocity u_* can be determined from $u_* = \langle(\epsilon\kappa z)^{1/3}\rangle$ (Dewey and Crawford 1988) where angle brackets denote a vertical average over the boundary layer and horizontal average over the bank, z is the vertical coordinate, and $\kappa = 0.4$ is von Kármán's constant. Our measurements indicate $\tau_b \simeq 0.2$ N m^{-2} during the flow of the downslope current.

The skin friction is estimated directly as the areal average of the bed stress over the bank, $\int \tau_b\, dA \sim 4 \times 10^6$ N ($dA = 2000 \times 10\,000$ m^2).

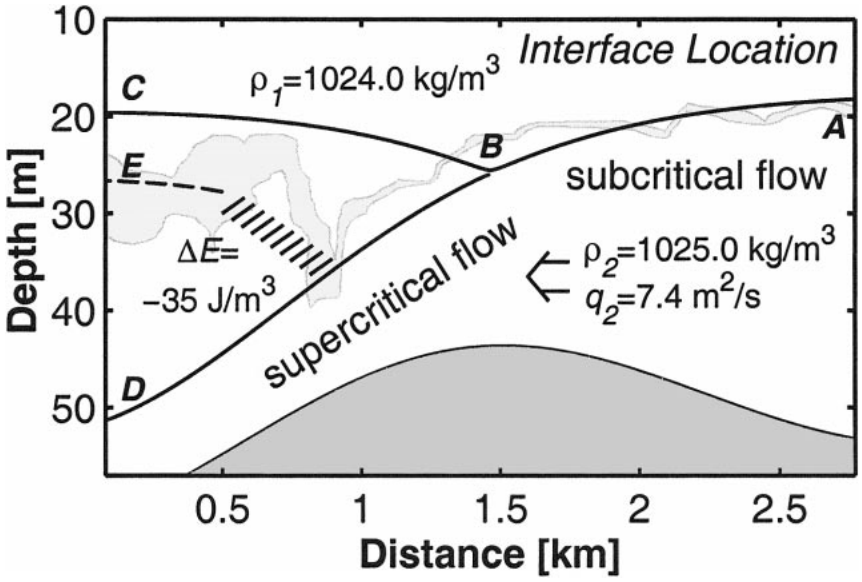

FIG. 3. Comparison of the observed interface height (represented by the shaded density range 1024.4–1024.6 kg m^{-3}) with the solutions of the hydraulic equations (solid lines). Path **AB** represents subcritical flow upstream of the bank, consistent with the observed interface height and measured Froude number. Path **BC** represents subcritical flow downstream of the bank that is inconsistent with both observed interface height and measured Froude number. Path **BD** represents supercritical flow downstream of the bank. This is consistent with both measured Froude number and the observed interface height to ~0.8 km, where a transition occurred. We postulate this transition to be an internal hydraulic jump. The path denoted by **E** and the intersection of **BD** is drawn to follow the observed interface. This path represents an energy loss of $\Delta E \cong -35$ J m^{-3}, presumably to turbulence.

The form drag is determined by the pressure drop across the bank. It is computed by integrating the horizontal component of pressure, p along the surface of the bank, $b(x)$, or

$$F_d = \int p(b)\frac{db}{dx}dA, \tag{1}$$

where $dA = dxdy$ (Baines 1995). This may be calculated directly from the two-layer hydraulic flow simulations, and is $\sim 13 \times 10^6$ N. Alternatively, F_d is estimated directly from the observed density, with the caveats that pressure is hydrostatic and the free surface pressure gradient is zero. The bounds on the latter estimate are 11–18 ($\times 10^6$ N).

The force exerted on the flow can be compared to the dominant dynamical terms governing its motion. During the upwelling season (spring/summer), alongshore currents are in geostrophic equilibrium. The dominant term is ρfU, where f is the Coriolis parameter (10^{-4} s^{-1} at 45°N). At the time of our observations over Stonewall Bank, U was about 0.2 m s^{-1}. Integrated over the volume of fluid over the bank, the total force on the flow over the bank is about 16×10^6 N. This is approximately the sum of skin friction plus form drag.

We might also consider the deceleration of the flow due to the bank drag. Comparing the local acceleration with the total drag, the decay timescale is $\tau = \rho U \delta \mathcal{V}/F_d$. The result is $\tau \sim 4$ h.

5. Mixing

We used two methods to estimate the eddy diffusivity: i) from TKE considerations ($K_\rho = \Gamma\epsilon/N^2$) (Osborn 1980), where Γ is thought to be $\simeq$0.2 (Moum 1996), $N^2 = -(g/\rho)\rho_z$, and (ii) from the thermal variance equation $K_T = \chi_T/2(T_z)^2$ (Osborn and Cox 1972), where T_z is the local vertical temperature gradient. The two methods are consistent and the results are summarized in terms of K_ρ (Fig. 4).

The increase in K_ρ downstream across the bank is large and significant (Fig. 4). Estimates of turbulence diffusivities upstream of the bank (dark shaded distribution in Fig. 4) are $\sim 10^{-5}$ m^2 s^{-1}, which we consider to be representative of background levels over the shelf. These values are no different from those found in the open ocean thermocline (NATRE: Ledwell et al. 1993), or from the shelf thermocline off Vancouver Island (Crawford and Dewey 1989) and the east coast of the United States during the recent Coastal Mixing and Optics Experiment (results from a dye tracer release: J. R. Ledwell 1999, personal communication) (Fig. 4). This would seem to confirm previous estimates of background levels of mixing over the shelf. However, immediately downstream of the bank, the mean value of K_ρ is more than 100 times greater.

The influence of such mixing events relative to the shelf as a whole can be noted by comparing the dia-

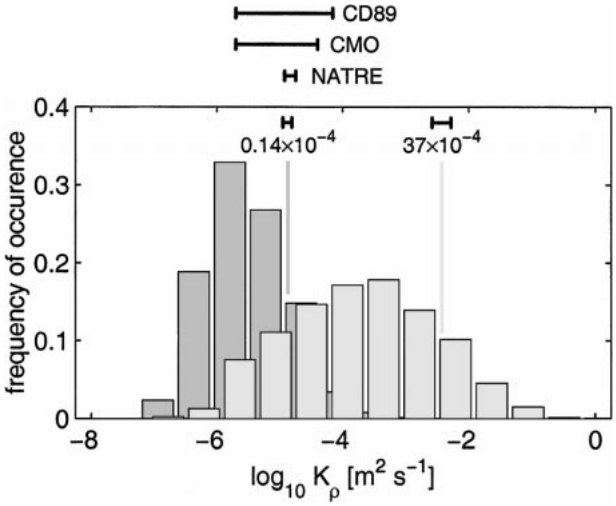

FIG. 4. Distributions of K_ρ upstream (dark) and downstream (light) of Stonewall Bank. Downstream refers to distances 500–1200 m in cross-bank coordinates (Fig. 2). Upstream is >2000 m. Mean values and 95% bootstrap confidence limits from these two distributions are shown within the box. Above the box are results from the ocean thermocline (NATRE) (Ledwell et al. 1993), the continental shelf off Vancouver Island (CD89) (Crawford and Dewey 1989), and the Mid-Atlantic Bight, which was the site of the Coastal Mixing and Optics Experiment (CMO) (J. R. Ledwell 1999, personal communication).

pycnal buoyancy flux integrated over the bank, J_bA, to that integrated over the greater shelf, $J_{b_0}A_0$. Here $J_{b_0} = K_{\rho_0}N_0^2$, $K_{\rho_0} = 10^{-5}$ m^{2}s^{-1}, and N_0^2 represents the buoyancy frequency over the shelf. Here A_0 is the greater shelf area and A is the area of the bank ($\sim 2 \times 10^7$ m^2); J_b is the buoyancy flux at the bank, $= K_\rho N^2$, where $K_\rho \sim 4 \times 10^{-3}$ m^{2}s^{-1}, and $N^2 \sim N_0^2$. The greater shelf area required to perform the same mixing as is accomplished over the bank can be estimated by considering the scenario in which the turbulence at Stonewall Bank accounts for all of the modification of shelf water by mixing (equivalent to setting $J_{b_0}A_0 = J_bA$: Lueck and Mudge 1997). This yields $A_0 \cong AK_\rho/K_{\rho_0}$, or 400 times the area of the bank. This area is roughly equivalent to the entire Oregon shelf to the 100-m isobath.

6. Discussion

Our observations suggest the importance of hydraulically controlled flow to fundamental ocean circulation. Studies in Knight Inlet (Farmer and Armi 1999a,b) and the Strait of Gibraltar (Wesson and Gregg 1994) have established the importance of hydraulic flows over sills in protected fjords and straits. Similarities of these flows to that over Stonewall Bank are striking. Using a combination of acoustic imaging and high-resolution Doppler profiling, details of the Knight Inlet flow were made clear that we cannot infer from our observations. Direct measurements of the downslope current indicated peak speeds in excess of 1.2 m s^{-1}. Trapped interfacial waves were observed upstream of the sill and shear instabilities at the plunging interface over the sill. The latter suggests that energetic turbulence should also be present. In turn, the Knight Inlet observations support the notion that our observation of high ϵ at the sheared top of the density current is due to shear instability. Since negligible cross-track flow of the active layer was observed, our two-dimensional analysis seems justified at this stage (and follows that of Farmer and Armi 1999b). However, Stonewall Bank is obviously three-dimensional and this must be considered an issue toward further understanding of the flow (Hunt and Snyder 1980).

The large drag induced on the flow over Stonewall Bank is analogous to mountain drag, to which Baines (1995) attributes 50% of the total drag on the atmosphere, as form drag over a small percentage of the earth's surface. The remaining 50% is frictional drag in the surface boundary layer, integrated over the earth's surface. Parameterization of mountain drag in atmospheric GCMs is a critical issue and an active area of research (e.g., PYREX experiment: Bougeault et al. 1997).

To be included in ocean models, the frequency and spatial occurrences of hydraulic flows must be understood. Measurements made over a 24-h period at the same location two days previously showed no obvious signs of hydraulically controlled flow or such highly energetic turbulence as observed here. In April 1999, we were able to again make a series of transects (over 14 hours) at the same location and with the same measurement setup. Preliminary analysis indicates the turbulence to be considerably more energetic with a faster downslope current flowing SSW (as in April 1998) over the bank. Perhaps the observation discussed here represents a moderate example of irregularly occurring hydraulic flow. Further analysis of the existing data and further study will be required to determine the range of flow conditions and the rate at which hydraulic flows occur over the bank.

The typical background flow over the shelf is a combination of baroclinic tidal and inertial oscillations, and barotropic coastal current. Current meters at 23 and 63 m below the surface in 80-m water depth (from the Coastal Upwelling Experiment: Pillsbury et al. 1974) have revealed semidiurnal tidal currents north of Stonewall Bank with peak-to-peak amplitudes 0.2–0.3 m s^{-1} that are 180° out of phase, providing velocity differences up to 0.6 m s^{-1} over 40 m vertically. It is certainly possible that the observed flow over Stonewall is set up regularly at tidal intervals, just as at Knight Inlet. However, the upstream–downstream density difference in the bottom layer is not available at Stonewall in the same way it is for a fjord flow. This may complicate the generation process. Alternatively, the flow may be set up by relaxation/intensification of the up/downwelling flows that are a feature of the Oregon coastal circulation in response to impulsive wind events such as we observed.

Enhanced mixing at a localized region rather than

weak mixing over a broad region of the shelf may be critical to the formation of the coastal jet produced by spring/summer upwelling (Dewey and Moum 1990). Characterized by strong horizontal density gradients, the coastal jet is formed near the coast during spring upwelling and moves offshore during sustained upwelling winds. Two scenarios arise, each representing a different phase in the evolution of the coastal jet. Mixing dense fluid upward offshore of the front (when the front is inshore of the bank) weakens the front, impeding the formation of the coastal jet. In contrast, when the front is offshore of the bank, the denser fluid raised up there will act to strengthen the front. In this way, once the front has passed seaward over the bank, it may be intensified and, by geostrophy, accelerated.

These observations highlight the problem of using spatially and temporally uniform values of K_ρ in numerical simulations. We have suggested reasons why spatial and temporal intermittency must be adequately resolved to predict the dynamics of coastal currents. We suspect that enhanced turbulence activity is associated with other features on the shelf and that it is likely that small topographic features induce a substantial fraction of the drag and mixing on the continental shelf.

Acknowledgments. This research was funded by the Office of Naval Research. We are grateful to Gunnar Gunderson for processing the ADCP data; to Mike Neeley-Brown, Ray Kreth, and Mike Zelman for technical support; and to Doug Caldwell, Jane Huyer, Bill Smyth, and John Toole for comments.

REFERENCES

Bacmeister, J., and R. Pierrehumbert, 1988: On high-drag states of nonlinear stratified flow over an obstacle. *J. Atmos. Sci.,* **45,** 63–80.

Baines, P. G., 1995: *Topographic Effects in Stratified Flows.* Cambridge, 482 pp.

Bougeault, P., B. Benech, P. Bessemoulin, B. Carissimo, A. J. Clar, J. Pelon, M. Petitdidier, and E. Richard, 1997: PYREX: A summary of findings. *Bull. Amer. Meteor. Soc.,* **78,** 637–650.

Crawford, W. R., and R. K. Dewey, 1989: Turbulence and mixing: Sources of nutrients on the Vancouver Island continental shelf. *Atmos.–Ocean,* **27,** 428–442.

Dewey, R. K., and W. R. Crawford, 1988: Bottom stress estimates from vertical dissipation rate profiles on the continental shelf. *J. Phys. Oceanogr.,* **18,** 1167–1177.

——, and J. N. Moum, 1990: Enhancement of fronts by vertical mixing. *J. Geophys. Res.,* **95,** 9433–9445.

Farmer, D. M., and R. A. Denton, 1985: Hydraulic control of flow over the sill in Observatory Inlet. *J. Geophys. Res.,* **90** (C5), 9051–9068.

——, and L. Armi, 1999a: The generation and trapping of solitary waves over topography. *Science,* **283,** 188–190.

——, and ——, 1999b: Stratified flow over topography: The role of small scale entrainment and mixing in flow reestablishment. *Proc. Roy. Soc. London,* **455A,** 3221–3258.

Hunt, J. C. R., and W. H. Snyder, 1980: Experiments on stably and neutrally stratified flow over a model three-dimensional hill. *J. Fluid Mech.,* **96** (4), 671–704.

Huyer, A. J., 1983: Coastal upwelling in the California Current system. *Progress in Oceanography,* Vol. 12, Pergamon Press, 259–284.

Ledwell, J. R., A. J. Watson, and C. S. Law, 1993: Evidence for slow mixing across the pycnocline from an open-ocean tracer-release experiment. *Nature,* **364,** 701–703.

Lueck, R. G., and T. R. Osborn, 1985: Turbulence measurements in a submarine canyon. *Contin. Shelf Res.,* **4** (6), 681–698.

——, and T. D. Mudge, 1997: Topographically induced mixing around a shallow seamount. *Science,* **276,** 1831–1833.

Moum, J. N., 1996: Efficiency of mixing in the main thermocline. *J. Geophys. Res.,* **101** (C5), 12 057–12 069.

——, M. C. Gregg, R. C. Lien, and M. E. Carr, 1995: Comparison of turbulence kinetic energy dissipation rate estimates from two ocean microstructure profilers. *J. Atmos. Oceanic Technol.,* **12,** 346–366.

Osborn, T. R., 1980: Estimates of the local rate of vertical diffusion from dissipation measurements. *J. Phys. Oceanogr.,* **10,** 83–89.

——, and C. S. Cox, 1972: Oceanic fine structure. *Geophys. Fluid Dyn.,* **3,** 321–345.

Pillsbury, R., J. Bottero, R. Still, and W. Gilbert, 1974: A compilation of observations from moored current meters; Vol. iv; Oregon continental shelf; April-October 1972. Data Rep. 57, Oregon State University, Corvallis, OR, 126 pp. [Available from College of Oceanic and Atmospheric Sciences, Oregon State University, Ocean. Admin. Bldg. 104, Corvallis, OR 97331-5503.]

Toole, J. M., R. W. Schmitt, K. L. Polzin, and E. Kunze, 1997: Near-boundary mixing above the flanks of a midlatitude seamount. *J. Geophys. Res.,* **102** (C1), 947–959.

Wesson, J. C., and M. C. Gregg, 1994: Mixing at Camarinal Sill in the Strait of Gibraltar. *J. Geophys. Res.,* **99** (C5), 9847–9878.

Zülicke, C., E. Hagen, and A. Stips, 1998: Dissipation and mixing in a coastal jet: A Baltic Sea case study. *Aquat. Sci.,* **60** (3), 220–235.